2D Materials

A direct transfer solution for digital laser printing of CVD graphene

To cite this article before publication: Symeon Papazoglou *et al* 2021 *2D Mater.* in press https://doi.org/10.1088/2053-1583/ac1ab6

A direct transfer solution for digital laser printing of CVD graphene

Symeon Papazoglou[1], Dimitrios Kaltsas[1], Adamantia Logotheti[1], Amaia Pesquera[2], Amaia Zurutuza[2], Leonidas Tsetseris[1], Ioanna Zergioti[1*]

[1]School of Applied Mathematical and Physical Sciences, National Technical University of Athens, Iroon Polytehneiou 9, 157 80, Athens, Greece
[2]Graphenea Headquarters, Paseo Mikeletegi 83, 20009 - San Sebastián, Spain
*corresponding author

Keywords: Laser Induced Forward Transfer, CVD growth, graphene, Raman mapping, Ab-Initio Molecular Dynamics

Abstract

State-of-the-art methods for printing highly resolved pixels of two-dimensional (2D) materials on technologically important substrates typically involve multiple and time-consuming processing steps which increase device fabrication complexity and the risk of impurity contamination. This work introduces an alternative printing approach based on the Laser Induced Forward Transfer (LIFT) technique for the successful digital transfer of graphene, the 2D material par excellence. Using LIFT, CVD graphene pixels of 30 μm x 30 μm in size are transferred on SiO_2/Si and flexible polymer substrates. The potential of upscaling this novel approach by reaching sizes of up to 300 μm x 300 μm for transferred graphene patches is also demonstrated. The feasibility of laser-induced transfer of graphene is corroborated with ab initio molecular dynamics simulations which elucidate atomic-scale details of the seamless detachment of the monolayer from a metallic donor surface and its subsequent attachment to a receiver substrate.

1. Introduction

Significant advances in recent years have ushered technology in the new era of additive manufacturing (AM) of devices for a wide range of applications. One of the most exciting AM fields is that of printed electronics, which, already at its nascent stage, has demonstrated its potential for the development of large-area, low-cost devices [1], for example, Radio Frequency Identification (RFID) sensors [2,3], touch [4,5] and wearable sensors and transistors [6,7]. The preparation of advanced electronic systems with printing techniques has key advantages over competing methods, such as decisively simpler and fewer processing steps, reduced post-processing waste, and the ability of transferring the materials of interest on either rigid or flexible substrates. By the same token, to harness the full potential of printed electronics, innovative solutions are required on how to suppress defect formation during transfer and enhance the resolution of printed patterns down to sub-micron scale, without compromising the potential for upscaling. These challenges are particularly acute in the case of two-dimensional (2D) materials (e.g. graphene), whose intriguing properties and delicate structures are generally more susceptible to degradation when they are subjected to common types of physical and chemical treatments in established transfer techniques [8,9].

To date, the most widely used methods to transfer graphene grown with Chemical Vapor Deposition (CVD) on metal substrates involve multiple processes, each carrying its own risk for unwanted modification, or even destruction of the printed specimen. Examples of such risky steps in the so-called wet-transfer methods are the chemical removal of any polymer employed as temporary support layer, the etching of the supporting metal foil (e.g. Cu, Ni), the transfer of graphene to the substrate of choice, and, finally, the removal of any solvent residues through high-temperature annealing [10,11]. On the other hand, solvent-free dry-transfer approaches have their own challenges to meet, e.g., the complete removal of any polymer stamps which may be used to facilitate the transfer [12,13], or the control of damage caused by the physical delamination of graphene when it is peeled off a metal substrate [14,15]. Furthermore, even if a relatively clean transfer is achieved by any means, the design of advanced printed electronics with high level of architectural complexity and functionality

poses yet another challenge, that of obtaining well-defined and site-specific transferred patterns. For this matter, photolithography can provide good control over printed features, but, unfortunately, it also increases the cost of the overall fabrication and the likelihood of impurity insertion during the removal of polymer photoresists [16].

Based on the above, there is clearly a need to bring in alternative methods for the fabrication of electronics utilizing 2D materials. Here, we demonstrate the potential of the Laser Induced Forward Transfer (LIFT) technique to set a new paradigm for the seamless and digital transfer of graphene and, possibly, other 2D materials. The LIFT approach has a long history and an impressive record of printing a broad range of materials e.g., metals [17], fullerene (C_{60}) crystallites, carbon nanotubes [18], polymer/carbon nanotube composites [19] and graphene oxide films [20]. In this relatively simple one-step process a laser pulse can force a controlled amount of the material of interest to detach from a so-called donor substrate (or, simply, donor) and be transferred to a receiver substrate forming pixels whose size and form are determined by the geometrical features of the laser spot. The underlying physical mechanisms involve typically the absorption of laser energy by the electrons of the donor, transfer of this energy to the lattice, rapid heating of the donor, generation of a pressure wave that leads to the expansion of its subsurface area and eventual ejection of surface material towards the receiver [21]. Often, an intermediate layer, called Dynamic Release Layer (DRL), is placed between the donor substrate and the material under transfer to facilitate the absorption of laser light at particular wavelengths [22]. Given that these surface phenomena can be highly destructive (unless they are tuned properly), it is not a priori clear that the technique can be used to transfer atomic-thick layers in their pristine form.

To open the way for the versatile LIFT approach to find wide application on the dry printing of delicate two-dimensional materials (without any simultaneous co-deposition of other, e.g., support materials), there is a need to demonstrate that such transfer is not just feasible, but that it can also be of high quality. In order to take real advantage of laser-induced printing in the fabrication of devices, spatial resolution of transferred patches down to the sub-micron scale and the ability of printing on-

demand arrays of largely defect-free pixels are sine-quo-non requirements, which, to our knowledge, have not been met yet for graphene or any other 2D material. On the first issue of feasibility, there has been a limited number of encouraging and highly motivating previous studies which reported laser-induced transfer of graphene, albeit together with a polymer support. For example, in previous notable experiments, Smits et al. [23] and Yoo et al. [24] used laser-induced transfer techniques to co-transfer single layers of graphene together with a thin polymer (PMMA) layer. More recently, Praeger et al. demonstrated the transfer of graphene using the Laser Induced Backward Transfer (LIBT) technique, however without being able to transfer a concrete, non-fragmented pixel and without avoiding the introduction of defects during the printing process that downgraded the quality of the transferred graphene [25]. Another example includes the laser transfer of crumpled fragments of CVD graphene using a blister-based laser transfer method by Komlenok et al. [26]. It is worth mentioning that lasers play a vital role in the synthesis of graphene also through the so-called Laser-Induced Graphene (LIG) method [27, 28]. By irradiating polymers with suitable laser light, the LIG method typically produces bulky graphene samples at reduced processing time and cost, but it is inferior to CVD when it comes to the preparation of high-quality single- or few-layer graphene. While these first attempts to transfer graphene with laser-based techniques are exciting and encouraging, the litmus test for any new AM technique is the successful printing of defect-free pixels in a controlled and scalable way. In this work, we show that it is possible, under the right conditions, to forward transfer solely graphene, and avoid the undesired co-transferring of any polymer films or DRL fragments. We thus demonstrate the first case of digital printing of this archetypal 2D material with high resolution (μm) on technologically important SiO_2/Si and flexible polydimethylsiloxane (PDMS) substrates, without the need of post-transfer processing steps. The term “high resolution” in this study refers to the well-defined dimensions and shape of the printed graphene pixels. It should be noted at this point that the growth of graphene by CVD on Ni films with thicknesses smaller than 100 nm is a challenge. The root of the problem pertains to the enhanced evaporation of Ni and solubility of C at the high temperatures required for the growth in the ultrathin case.

On the theory side, the possibility of using intense light to pattern graphene or exfoliate it from graphite has been probed with Molecular Dynamics (MD) simulations. For example, Xiong et al. [29] employed classical MD calculations coupled with the so-called two-temperature model to describe how ultrafast lasers can pattern graphene with desired nano-grooves through ablation. Moreover, Jeschke et al. [30] showed with MD studies based on the tight-binding method that, under conditions simulating fs laser pulses, intact graphene sheets can be removed from graphite. A similar conclusion was reached using ab initio MD techniques by Miyamoto and coworkers for the so-called photo-exfoliation of graphene from graphite [31]. On the other hand, the main topic of the present work, i.e. transfer of graphene from a donor metallic surface to a dielectric substrate has not received, to our knowledge, any dedicated theoretical attention so far. We have thus employed ab initio Molecular Dynamics (AIMD) simulations to confirm that, when the right amount of energy is deposited by a laser on a metallic (Ni) substrate with a graphene overlayer, the latter can be ejected from the Ni surface and get then attached to a SiO_2 receiver, without any defects or impurities formed on the graphene sheet during the whole process.

2. Experimental methods

Preparation of LIFT donor substrates

Graphene was grown on a poly-crystalline copper (Cu) foil catalyst (18 μm) via chemical vapor deposition using a Cold Wall CVD Reactor from Aixtron. The Cu foil was chemically treated and thermally annealed prior to the graphene growth at 1000 °C and at low pressure using methane as the carbon source. The graphene was transferred from the Cu foils to Ni coated (50 nm) quartz substrates using a standard wet transfer process where a poly(methyl methacrylate) (PMMA) layer is first applied onto the graphene/Cu followed by etching of the Cu foil. After cleaning the PMMA/graphene film in water to remove any excess Cu etching solution, the film is placed on the Ni coated quartz substrate by submerging the substrate in water. Finally, the PMMA is removed using acetone.

LIFT experimental setup

Laser printing experiments were performed using an in-house developed laser printing setup. The 3rd harmonic of a pulsed Nd:YAG (8 ns) laser in single-shot mode was employed for all printing experiments. The experiments were performed at the image plane and a square mask was used to produce a demagnification ratio of 0.015 and to enable the projection of a 2 mm x 2 mm square into a 30 μm x 30 μm square at the image plane located 450 μm below the focal point of the objective lens (30 mm focal length). A number of experiments were carried out under reduced pressure conditions (few tens of mbar), generated from a rotary pump (Alcatel Adixen), using a custom-made vacuum cage and a digital Pirani gauge to monitor the pressure during printing. The donor and the receiver substrates were kept at near contact throughout the printing process.

Ab Initio Molecular Dynamics Simulations

For Ab Initio Molecular Dynamics (AIMD) simulations we used the code Vienna Ab initio Simulation Package (VASP), the Perdew–Burke–Ernzerhof (PBE) exchange-correlation functional, projector augmented waves, and the DFT-D2 method, to include van der Waals interactions. A detailed description can be found in the supplementary material.

Characterization

Micro-Raman spectra have been recorded using the Renishaw inVia Reflex microscope operating at 514 nm using a 50x objective lens with 0.8 μm laser spot diameter on the sample. The laser power was kept at 0.3 mW to avoid heating of the material during the measurements. Raman spectra were collected within the 1000-3200 cm^{-1} region and acquisition time was 10 s with 2 accumulation rounds for each spectrum. SEM measurements have been performed using the ultra-high resolution JEOL JSM-7401f Field Emission Scanning Electron Microscope (FESEM), with an accelerating voltage ≤ 2 kV. The samples have been characterized without any prior metallization step. AFM measurements have been performed using the Veeco diInnova 840-012-711 operating at tapping mode.

3. Results and discussion

Since previous attempts to transfer graphene using laser pulses resulted in, either graphene co-transferred with protective layers (e.g. PMMA) [23,24], or irregular and defective patterns [25,26],

we focused on identifying the key parameters that would preserve the shape and quality of graphene after transfer. For the laser printing experiments, the quartz/Ni/graphene configuration is used as donor substrate (Figure 1). Ni is not the only metal which can be applied on the donor substrate to facilitate the transfer since other refractory metals can be used as well. It was selected in the present work because it absorbs the incoming laser wavelength (355 nm) and can thus trigger the initial stage of the transfer.

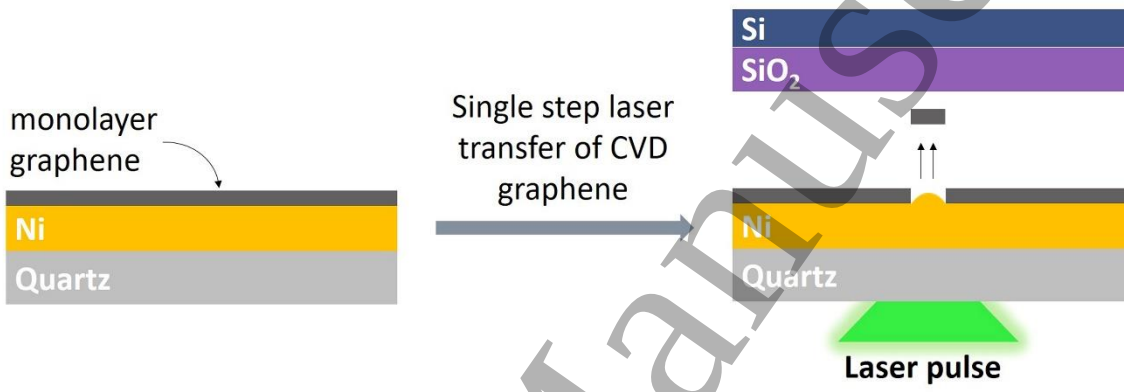

Figure 1. Schematic representation of single step laser transfer of CVD graphene. CVD grown graphene is placed on a quartz/Ni substrate. A laser pulse is then projected on the Ni Dynamic Release Layer and transfers a selected part of single layer graphene on the surface of the SiO_2/Si substrate.

The applied laser energy density (E_l) is an important factor that enables successful deposition within an optimum window between two threshold values. Below the lower threshold E_l, no transfer occurs. In our case, i.e. for single layer graphene on Ni, this minimum E_l is measured at 20 mJ/cm^2, whereas slightly higher values (30 mJ/cm^2) lead to partial transfer (supplementary material Fig. S1a). On the other hand, energy densities above the upper limit of 100 mJ/cm^2 result to violent ablation of Ni and the transferred species are predominantly melted Ni nanoparticles (supplementary material Fig. S1b). Hence, the optimum energy density window is determined in the range between 40-80 mJ/cm^2 (sub-ablation regime) and the results described in the following were obtained with an E_l value of 50 mJ/cm^2. The parameter, however, we have identified as being the most crucial in achieving the first largely defect-free transfer of graphene is the pressure under which the experiment is performed. In

particular, when LIFT is attempted under atmospheric pressure, the graphene monolayer lands on the receiver substrate in fragments and exhibits significant levels of folding (supplementary material Fig. S2a, b). These results suggest that air resistance affects adversely the transfer of an atomic-thick layer of graphene.

On the contrary, experiments performed under a low pressure of few tens of mbar, achieve significantly better printing quality with uniform and continuous coverage of the receiver substrate by the transferred graphene monolayer (Figure 2a, b). Figure 2a, for instance, shows an array of laser printed graphene pixels onto a SiO_2/Si substrate (300 nm oxide thickness), with pixel size of 30 μm x 30 μm at a laser fluence of 50 mJ/cm^2. The printed pixels exhibit well-defined shapes that correspond to that of the projected laser beam. Further evidence in this regard is provided by the SEM image (Figure 2b) of a single graphene pixel of the array. In addition, detailed characterization with Raman spectroscopy confirms the high quality and monolayer form of these pixels.

As is known, the presence and relative intensities of the characteristic D, G and 2D peaks of graphene in Raman spectra can give a quantitative account for the number of layers and the concentration of defects in graphene samples [32,33]. Specifically, the peak intensity ratio of the 2D over the G peak (for single layer graphene usually >2) gives a simple and direct means to determine the number of graphene layers, while the D peak, a defect-induced peak, provides information related to the presence or absence of defects [33]. Figure 2d shows the Raman color map for the I_{2D}/I_G peak intensity ratio, reconstructed using 30 Raman measurements obtained from a single graphene pixel transferred on SiO_2/Si (30 μm x 30 μm). The average peak intensity ratio of the 2D over the G peak is calculated at 3.24±0.57 in accordance with the reference donor substrate's (quartz/Ni/graphene) I_{2D}/I_G ratio values (3.57±0.42, supplementary material Fig. S3). The average G peak position is at 1588.30±1.44 cm^{-1} and has a full width at half maximum (FWHM) of 12.25±1.62 cm^{-1}, while the average 2D peak position and FWHM are, respectively, 2689.77±1.65 cm^{-1} and 27.56±1.60 cm^{-1}.

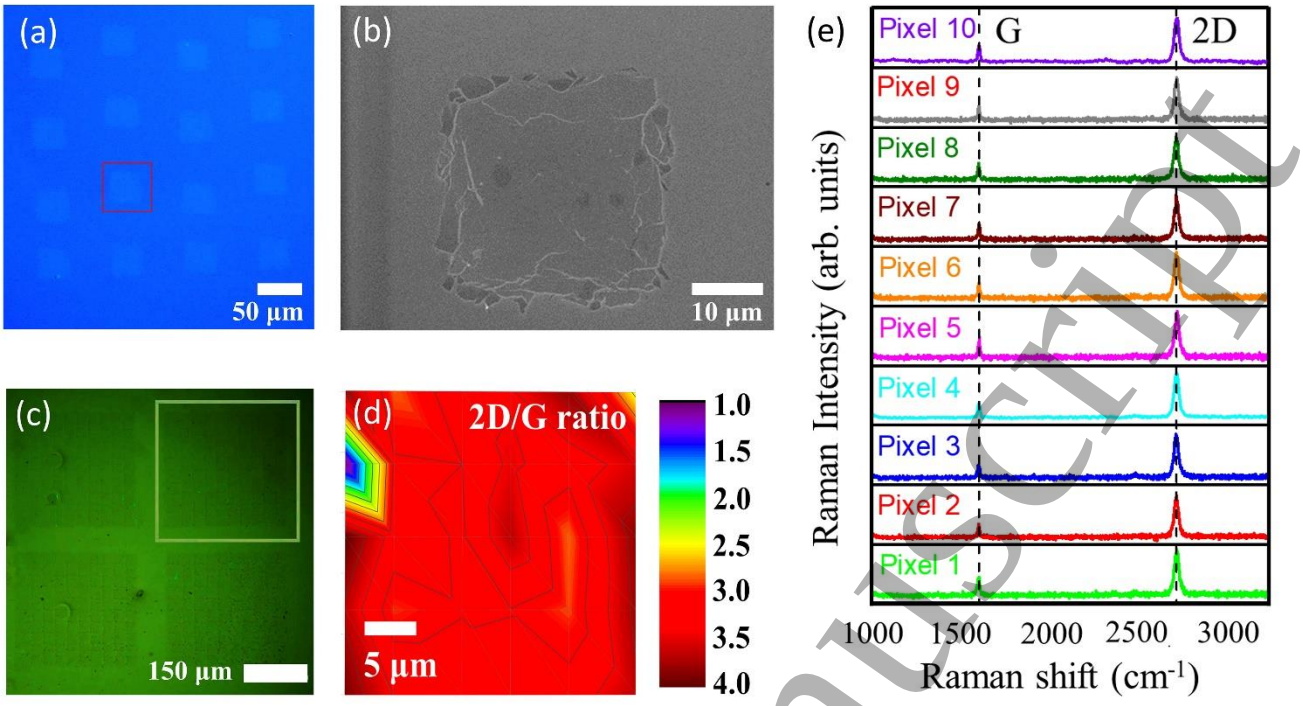

Figure 2. Laser printing of single layer CVD graphene on SiO_2/Si and PDMS and Raman color map of the printed graphene pixels. (a) Optical microscopy image of a laser printed graphene array on SiO_2/Si, (b) SEM image of graphene pixel highlighted in red in (a), (c) Optical microscopy image of 4 graphene arrays printed on PDMS and comprising 10x10 graphene pixels each, (d) Raman color map of I_{2D}/I_G peak intensity ratio within a single graphene pixel printed on SiO_2/Si (pixel 10 in (e)), € Raman spectra of 10 distinct laser printed graphene pixels on SiO_2/Si.

To investigate the reproducibility of the laser printing process, in terms of graphene uniformity as well as the layer structure and morphology among 100 LIFT printed graphene pixels (30 µm x 30 µm in size each), we employed micro-Raman spectroscopy. Figure 2e, presents Raman spectra from 10 distinct graphene pixels LIFT printed on SiO_2/Si and each spectrum corresponds to a single measurement taken from one random point within each pixel. In this case, the ratio comprising the average intensities of the 2D over the G peak is 3.00±0.31. The G (2D) peak has an average position at 1590.86±0.92 cm^{-1} (2692.01±1.01 cm^{-1}) and a FWHM of 13.00±1.14 cm^{-1} (29.60±1.17 cm^{-1}). The absence of the defect-induced D peak (~1350 cm^{-1}) [34], indicates that no noticeable defects are introduced during the laser transfer process. What is especially important for any technological application and for upscaling of the technique is the fact that these advantageous Raman results are

common to all 10 different pixels offering clear evidence that LIFT-induced deposition of graphene can be highly controllable and reproducible. The small deviation in the G and 2D peak positions between the average values from the different pixels lies within the range of fluctuations and due to unintentional electron or hole doping [34]. The Raman color map in Figure 2d demonstrates uniform monolayer graphene coverage of the SiO_2/Si substrate after laser printing, confirmed also through Atomic Force Microscopy (AFM) measurements (supplementary material Fig. S4), which were obtained under tapping mode operation and gave an average thickness of 0.4 nm for the laser printed graphene features. Apart from transferring onto a SiO_2/Si substrate, we have also achieved printing of graphene pixels on a flexible substrate, namely PDMS. Figure 2c displays four arrays of transferred graphene on PDMS. Each array comprises 100 graphene pixels and covers an area of approximately 300 μm x 300 μm (0.6 mm x 0.6 mm in total for the four arrays). Hence, the LIFT technique is suitable not only for transferring graphene with high resolution (printed graphene pixels 15 μm x 15 μm in size can be seen in supplementary material Fig. S5) but also for the coverage of larger -millimeter size- areas with single layer graphene patterns. The compatibility with PDMS also proves that the process can be combined with temperature sensitive substrates which are important in printed electronics applications.

The experimental demonstration of laser-induced transfer of graphene poses, in turn, the challenge of establishing also a theoretical proof-of-principle for this process. In particular, there is a challenge to identify mechanisms which can be triggered when a laser deposits the right amount of energy on a metallic (Ni) substrate and enables the detachment of a graphene overlayer in a defect- and impurity-free form. To this end, we have performed AIMD simulations within the Density Functional Theory (DFT) approach, one of the best tools to probe the atomic-scale phenomena of interest with high accuracy. Details of the method can be found in the supplementary material. Even though the interaction of laser light with matter in LIFT experiments is a very complex phenomenon [22,35], with electronic and lattice excitations happening at multiple time and length scales (the study of which is beyond the scope of DFT), the decisive final step that could trigger the ejection of a 2D overlayer

pertains to the arrival of the laser-induced pressure wave at the vicinity of the surface. In the present work, we focus exactly on this key stage and model the front of the wave by adding to the thermal velocities of atoms in the third subsurface layer of Ni an extra velocity component in the z-direction as described in the SI. In this way, we can adjust the areal density E_{in} of the excess kinetic energy (i.e. in addition to the thermal energy) the subsurface area acquires when the laser-induced wave arrives. Given that the laser deposits its energy in a much larger part of the donor, E_{in} has to be only a small fraction of the laser fluence applied in the experiments in order for the simulations to be realistic.

The main findings of the AIMD simulations are presented in Figure 3 where three different scenarios are identified depending on E_{in} (in the SI we provide corresponding movies with full details of the processes described below). In particular, for a low E_{in} value of 0.37 mJ/cm^2 (Figure 3a) the outward expansion of the subsurface area pushes the graphene overlayer to a maximum average distance of 3.5 Å away from the surface of Ni, but fails to instigate transfer of graphene as the latter eventually relaxes back to the initial physisorbed configuration. In contrast, for a large E_{in} value of 2.30 mJ/cm^2 (Figure 3c), the graphene overlayer is pushed away from the surface, but, a significant number of Ni surface atoms are also ejected from the metallic surface and fly away as unwanted adatom impurities on graphene.

The most important result, however, is obtained for an intermediate E_{in} value of 0.47 mJ/cm^2. In this case, and as shown in Figure 3b, a defect- and impurity-free graphene monolayer reaches, after 2400 fs from the initial time t_0 of the simulation, an average distance of about 11 Å away from the surface. At this point, the overlayer can be considered as fully detached because interactions with the Ni surface practically vanish at such large separation distances. We note that this optimal E_{in} value (0.47 mJ/cm^2) is a small fraction of the experimental fluences (40-80 mJ/cm^2) needed for successful transfer. Given that the energy is deposited by the laser on a much bigger volume of the metallic substrate than the one corresponding to the initial velocity field described above, the fact that the calculated E_{in} value is a portion of the experimental fluence required for transfer strengthens further the AIMD results as a theoretical proof-of-concept.

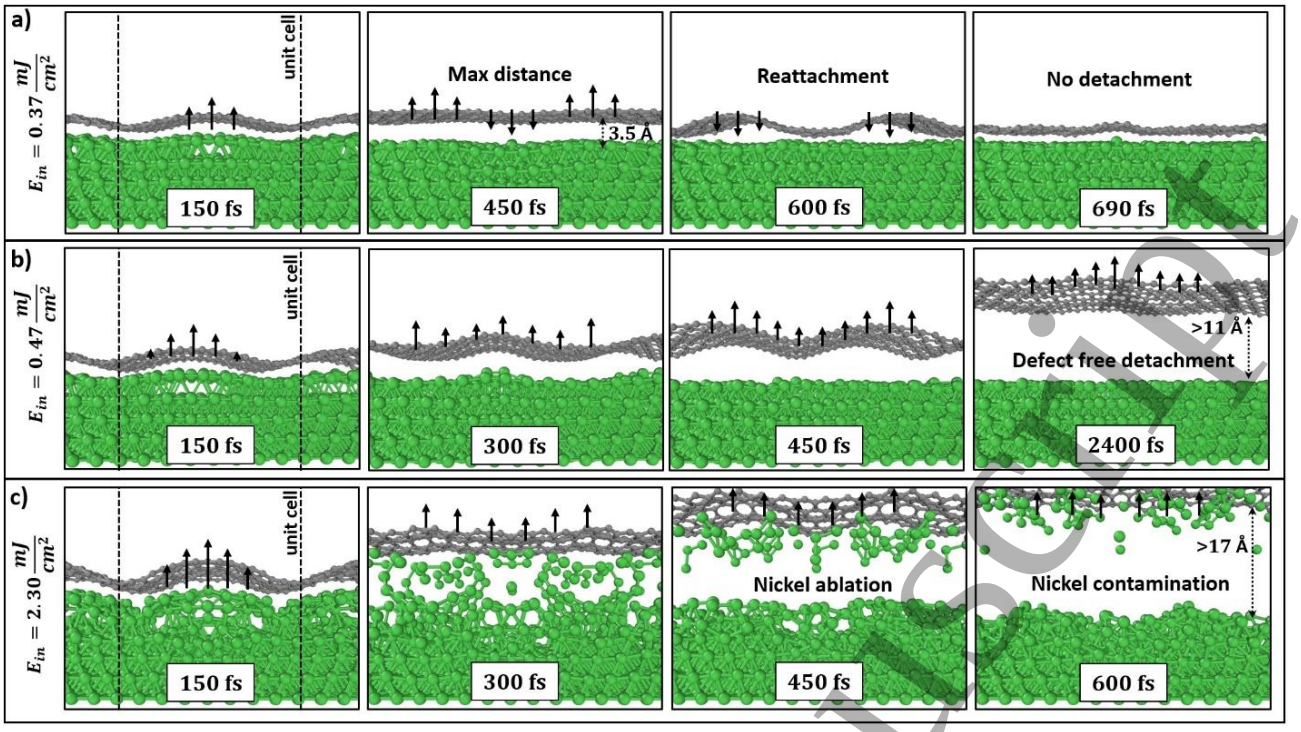

Figure 3. Snapshots depicting the evolution of the graphene/Ni system at different timesteps during AIMD simulations. The initial excess kinetic energy in the subsurface area is (a) 0.37 mJ/cm^2, (b) 0.47 mJ/cm^2 and (c) 2.30 mJ/cm^2. [Ni: green, C: grey spheres].

The center of mass of the ejected graphene monolayer shown in Figure 3b moves with a speed of 220 m/s. This value falls within the range of measured ejection velocities in various LIFT experiments, validating to a certain extent the approximations we employed in modelling the deposited energy in the subsurface area [36,37]. Using the exact same configuration of Figure 3 (in terms of position and velocity of each graphene atom) as input, we performed a second round of AIMD simulations, whereupon the detached graphene monolayer arrives at a SiO_2 receiver substrate. When the graphene sheet hits the SiO_2 receiver, it undergoes rapid equilibration to a practically flat configuration with an average distance of 3 Å from the receiver (Figure 4).

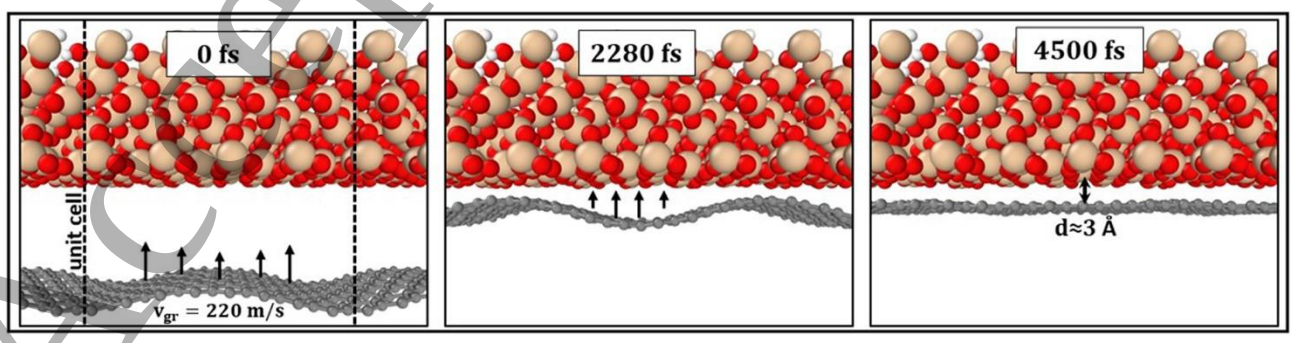

Figure 4. AIMD simulation snapshots depicting the approach and attachment of a graphene monolayer to a SiO_2 receiver substrate. The deposited graphene sheet equilibrates quickly to an approximately flat configuration which has an average distance d of 3 Å from the silica surface. [C: grey, Si: light orange, O: red, H: white spheres]

This last deposition step completes the picture emerging from the simulations, in agreement with the experimental results described above, on the feasibility of defect-free detachment of graphene from the donor and its smooth attachment on the receiver.

4. Conclusions

In summary, we have demonstrated the capacity of the LIFT technique to achieve the selective, defect-free and digital transfer of CVD-grown graphene without the need for post-printing processing steps. Raman color mapping and SEM characterization, along with high-level ab initio molecular dynamics simulations, revealed that LIFT can enable, in a reproducible manner, the seamless ejection of a graphene monolayer from a donor Ni surface and its attachment on a receiving SiO_2 or polymer substrate. We have thus shown that LIFT can meet key open challenges in the rapidly expanding field of printed electronics by offering a novel, cost-effective and time-efficient approach for the high-resolution transfer of two-dimensional materials both on conventional Si and flexible substrates.

ORCID iDs

Symeon Papazoglou https://orcid.org/0000-0002-4910-8018
Dimitrios Kaltsas https://orcid.org/0000-0001-8348-6971
Adamantia Logotheti https://orcid.org/0000-0003-1473-2141
Amaia Pesquera https://orcid.org/0000-0001-9700-8575
Amaia Zurutuza https://orcid.org/0000-0001-6376-0224
Leonidas Tsetseris https://orcid.org/0000-0002-0330-0813
Ioanna Zergioti https://orcid.org/0000-0001-6341-4495

Acknowledgements

This work was supported by the European Union's Horizon 2020 research and innovation programme under grant agreement No. 801389 (Project LEAF-2D). This work was supported by computational time granted from the Greek Research & Technology Network (GRNET) in the National HPC facility – ARIS – under project pr009016-CREAM. The authors would like to thank Dr. Doron Naveh and his group from Bar-Ilan University, Tel-Aviv for providing the Ni-coated quartz substrates for the

laser printing experiments. The authors would also like to thank Dr. Kontos, Dr. Arfanis and Dr. Falaras for providing access to the Raman characterization facilities of the Institute of Physical Chemistry of the NCSR Demokritos and Dr. Raptis and Ms. Skoulikidou for the SEM measurements at the facilities of the Institute of Nanoscience and Nanotechnology of the NCSR Demokritos.

Conflict of interest

The authors declare no competing interests.

References

1. Baumbauer C L et al. 2020 Printed, flexible, compact UHF-RFID sensor tags enabled by hybrid electronics *Sci. Rep*. **10 16543**

2. Singh R, Singh E, Nalwa H S 2017 Inkjet printed nanomaterial based flexible radio frequency identification (RFID) tag sensors for the internet of nano things *RSC Adv*. **7 48597-630**

3. Huang Q, Zhu Y 2019 Printing Conductive Nanomaterials for Flexible and Stretchable Electronics: A Review of Materials, Processes, and Applications *Adv. Mater. Technol*. **4 1800546**

4. Ma S et al. 2015 Fabrication of Novel Transparent Touch Sensing Device via Drop-on-Demand Inkjet Printing Technique *ACS Appl. Mater. Interfaces* **7 21628–633**

5. Lee W et al. 2015 A fully roll-to-roll gravure-printed carbon nanotube-based active matrix for multi-touch sensors *Sci. Rep*. **5 17707**

6. Shiwaku R et al. 2018 A Printed Organic Amplification System for Wearable Potentiometric Electrochemical Sensors *Sci. Rep*. **8 3922**

7. Matsui H, Takeda Y, Tokito S 2019 Flexible and printed organic transistors: From materials to integrated circuits *Org. Electron*. **75 105432**

8. Jabari E, Ahmed F, Liravi F, Secor E B, Lin L, Toyserkani E 2019 2D printing of graphene: a review *2D Mater*. **6 042004**

9. Liang X et al. 2011 Toward clean and crackless transfer of graphene *ACS Nano* **5 9144-53**

10. Kim K S et al. 2009 Large-scale pattern growth of graphene films for stretchable transparent electrodes *Nature* **10 706-10**

11. Johnson B et al. 2015 Institute of Photonic Sciences, Catalan Institution for Research and Advanced Studies, Corning (United States) US 9828285 B2

12. Seo J et al. 2018 Direct Graphene Transfer and Its Application to Transfer Printing Using Mechanically Controlled, Large Area Graphene/Copper Freestanding Layer *Adv. Funct. Mater.* **28 1707102**

13. Cha S, Cha M, Lee S, Kang J H, Kim C 2015 Low-Temperature, Dry Transfer-Printing of a Patterned Graphene Monolayer *Sci. Rep.* **5 17877**

14. Na S R et al. 2015 Selective Mechanical Transfer of Graphene from Seed Copper Foil Using Rate Effects *ACS Nano* **9 1325–35**

15. Moghadam F, Roh J S, Shin J E, Park H B 2020 *Sustainable Nanoscale Engineering: From Materials Design to Chemical Processing*, 1st Edition (Eds. G. Szekely, A. Livingston) Elsevier, Cambridge, MA, USA

16. Sul O, Kim K, Choi E, Kil J, Park W, Lee S B 2016 Reduction of hole doping of chemical vapor deposition grown graphene by photoresist selection and thermal treatment *Nanotechn.* **27 505205**

17. Koritsoglou O et al. 2019 Copper micro-electrode fabrication using laser printing and laser sintering processes for on-chip antennas on flexible integrated circuits *Opt. Mater. Expr*. **9 3046-58**

18. Goodfriend N T et al. 2018 Blister-based-laser-induced-forward-transfer: a non-contact, dry laser-based transfer method for nanomaterials *Nanotechn*. **29 385301**

19. Boutopoulos C, Pandis C, Giannakopoulos K P, Pissis P, Zergioti I 2010 Direct laser immobilization of photosynthetic material on screen printed electrodes for amperometric biosensor *Appl. Phys. Lett.* **96 041104**

20. Papazoglou S et al. In-situ sequential laser transfer and laser reduction of graphene oxide films 2018 *Appl. Phys. Lett*. **112 183301**

21. Delaporte P, Alloncle A P 2015 Laser-induced forward transfer: A high resolution additive manufacturing technology (invited) *Opt. Laser Technol.* **78 33-41**

22. Serra P, Pique A 2018 Laser Induced Forward Transfer: Fundamentals and Applications *Adv. Mater. Technol.* **4 1800099**

23. Smits E C P, Walter A, de Leeuw D M, Asadi K 2017 Laser induced forward transfer of graphene *Appl. Phys. Lett.* **111 173101**

24. Yoo J H, Park J B, Ahn S, Grigoropoulos C P 2013 Laser Induced Direct Graphene Patterning and Simultaneous Transferring Method for Graphene Sensor Platform *Small* **9 4269-75**

25. Praeger M et al. 2020 Laser-induced backward transfer of monolayer graphene *Appl. Surf. Sci.* **533 147488**

26. Komlenok M S et al. 2020 Printing of Crumpled CVD Graphene via Blister-Based Laser-Induced Forward Transfer *Nanomaterials* **10 1103**

27 Stanford M G et al. 2020 High-Resolution Laser-Induced Graphene. Flexible Electronics beyond the Visible Limit *ACS Appl. Mater. Interfaces* **12 10902–907**

28 Li G 2019 Direct laser writing of graphene electrodes *J. Appl. Phys.* **127 010901**

29. Xiong Q L, Sha Z D, Pei Q X, Kitamura T, Li Z H 2018 Thermal damage and ablation behavior of graphene induced by ultrafast laser irradiation *J. Therm. Stresses* **41 1153-68**

30. Jeschke H O, Garcia M E, Bennemann K H 2001 Theory for the Ultrafast Ablation of Graphite Films *Phys. Rev. Lett.* **87 015003**

31. Miyamoto Y, Zhang H, Tománek D 2010 Photoexfoliation of Graphene from Graphite: An Ab Initio Study *Phys. Rev. Lett.* **104 208302**

32. Ferrari A C, Basko D M 2013 Raman spectroscopy as a versatile tool for studying the properties of graphene *Nature Nanotechnol.* **8 235-46**

33. Ferrari A C et al. 2006 Raman Spectrum of Graphene and Graphene Layers *Phys. Rev. Lett.* **97 187401**

34. Casiraghi C, Pisana S, Novoselov K S, Geim A K, Ferrari A C 2007 Raman fingerprint of charged impurities in graphene *Appl. Phys. Lett*. **91 233108**

35. Mills B, Heath D J, Feinaeugle M, Eason R W 2018 *Laser Printing of Functional Materials: 3D Microfabrication, Electronics and Biomedicine*, (Eds: A. Pique, P. Serra), Wiley-VCH Verlag GmbH & Co. KGaA

36. Feinaeugle M, Alloncle A P, Delaporte Ph, Sones C, Eason R 2012 Time-resolved shadowgraph imaging of femtosecond laser-induced forward transfer of solid materials *Appl. Surf. Sci.* **258 8475-83**

37. Unger G, Gruene M, Koch L, Koch J, Chichkov B N 2011 Time-resolved imaging of hydrogel printing via laser-induced forward transfer *Appl. Phys. A* **103 271-77**